

The Effect of Cell Dimensions of Hydrated Mixed Metal Oxides with a Pyrochlore Structure on the Ion-Exchange Properties

Teresia Möller,^{*,†} Abraham Clearfield,[‡] and Risto Harjula[‡]

Laboratory of Radiochemistry, Department of Chemistry, P.O.Box 55, FIN-00014 University of Helsinki, Helsinki, Finland, and Department of Chemistry, Texas A&M University, College Station, Texas 77843

Received June 25, 2001. Revised Manuscript Received August 28, 2001

The relationship between the lattice parameter of the cubic unit cell and the ion-exchange properties was studied for a group of mixed metal oxides with the cubic pyrochlore structure, which had been prepared hydrothermally and by precipitation. The materials included binary oxides antimony silicate, antimony titanate, and titanium tungstate and related compounds, which contained a third metal (W^{6+} , Sb^{5+} , Nb^{5+}) in the framework structure that had been incorporated in an attempt to improve their ion-exchange properties. The lattice parameters were found to vary between 10.2440 and 10.4793 Å depending on the element combination and the cationic form of the material. A clear increase in the trace strontium (^{89}Sr) uptake in 0.1 M HNO_3 and 0.1 M $NaNO_3$ was observed when the lattice parameter was > 10.34 Å. A similar increase was found for alkaline earth metals at macro concentrations, but the increase was transient as the cubic unit cell dimensions were affected by the nature of the in-going cation. Some of the materials showed high selectivity for the alkaline earths against the H^+ ion making them suitable for removal of these cations from acidic solutions. However, the relative selectivity between the different alkaline earth cations was rather low in general, which does not allow for their selective individual separation. The three-dimensional tunnel structure of the pyrochlore showed clear ion sieve property in the separation of the relatively large Cs^+ cation from the other alkali metals.

Introduction

The group of materials known as hydrated metal oxides have been investigated extensively for use as ion exchangers.^{1–4} In general, the crystallinity of the hydrated metal oxide strongly affects its ion-exchange properties. The hydrated oxides of Sb^{5+} , W^{6+} , Nb^{5+} , and Ti^{4+} have traditionally been prepared in hydrolysis reactions at low temperature. The products are often amorphous but have good ion-exchange capacities. Hydrothermal treatment at < 200 °C usually improves the crystallinity of the product while still permitting them to retain their ion-exchange properties. Heating the hydrated metal oxides prepared at low temperatures to greater than 400 °C generally lessens their capacity. Furthermore, while it is possible to obtain highly crystalline materials via solid-state reactions at high temperatures (800–1200 °C), such materials seldom have significant ion-exchange capacities.

The recent hydrothermal preparation of $WO_3 \cdot 0.5H_2O$, which usually is synthesized at high temperatures, shows that pyrochlores can be prepared at lower temperatures as long as the pH is favorable.^{5–6} Another well-known pyrochlore is hydrated antimony pentoxide (antimonic acid) $Sb_2O_5 \cdot 4H_2O$ that has been prepared by hydrolysis.^{1,7} Its ion-exchange properties have been under extensive study, and a capacity of 5.1 mequiv g^{-1} has been determined.⁸ In addition, it has been found to tolerate a rather wide pH range and it has a high affinity for strontium in acidic conditions.^{9–11} These properties are beneficial when considering an ion exchanger for the treatment of nuclear waste effluents.

The cubic pyrochlore structure (general formula $A_2B_2O_6O'$, $Fd\bar{3}m$, $a \approx 10.3$ Å) may be crystallized under a broad range of synthetic conditions when the atoms A and B are of appropriate size and charge. The most typical charge combinations are (A^{3+} , B^{4+}) and (A^{2+} ,

* To whom correspondence should be addressed. E-mail: teresia.moller@helsinki.fi.

† University of Helsinki.

‡ Texas A&M University.

(1) (a) Clearfield, A. *Inorganic Ion Exchange Materials*; CRC Press: Boca Raton, FL, 1982. (b) Clearfield, A. *Chem. Rev.* **1988**, *88*, 125.

(2) Amphlett, C. B.; McDonald, L. A.; Redman, M. *J. Inorg. Nucl. Chem.* **1958**, *6*, 236.

(3) Kasuga, F.; Yamazaki, H.; Inoue, Y.; Tochiyama, O. *Bull. Chem. Soc. Jpn.* **1996**, *69*, 1275.

(4) Kasuga, F.; Yamazaki, H.; Inoue, Y. *Solvent Extr. Ion Exch.* **1996**, *14* (1), 161.

(5) Reis, K. P.; Ramanan, A.; Whittingham, M. S. *J. Solid State Chem.* **1992**, *96*, 31.

(6) Guo, J.-D.; Reis, K. P.; Whittingham, M. S. *Solid State Ionics* **1992**, *53–56*, 305.

(7) Abe, M.; Ito, T. *Bull. Chem. Soc. Jpn.* **1968**, *41*, 333; **1979**, *52* (5), 1386.

(8) Baetsle, L. H.; Huys, D. *J. Inorg. Nucl. Chem.* **1968**, *30*, 639.

(9) Konecny, C.; Kourim, V. *Radiochem. Radioanal. Lett.* **1969**, *2*, 47.

(10) Nonikov, B. G.; Materova, E. A.; Belinskya, F. A. *Russ. J. Inorg. Chem.* **1975**, *20*, 876.

(11) Zouad, S.; Jean Jean, J.; Loos-Neskovic, C.; Federoff, M.; Piffard, Y. *J. Radioanal. Nucl. Chem.* **1994**, *182*, 193.

B⁵⁺), with a radius of $0.87 < r_A < 1.51 \text{ \AA}$ for A and $0.40 < r_B < 0.78 \text{ \AA}$ for B. The pyrochlore structure is built up from corner-sharing BO₆ octahedra and an interpenetrating A₂O' chain that together create a three-dimensional framework. The A cations are eight-coordinated to the oxygens of the BO₆ octahedra and two O' atoms. The A and O' atoms of the A₂O' chain are not very essential in the stabilization of the basic structure, and vacancies may occur at both sites leading to defect pyrochlores. The tunnels of the pyrochlores are usually smaller than those of zeolites (4–7 Å). Water molecules and other charge-balancing cations are located in the tunnels and cavities of the framework.^{12–14}

Substitution of A and/or B leads to a practically unlimited number of mixed pyrochlores with different properties. Such substituted defect pyrochlores may possess properties, including interesting ion-exchange properties, not possessed by the stoichiometric counterparts. Substitution of a framework metal by another atom has already proven to be an important means in fine-tuning the ion-exchange properties of titanosilicates.^{15,16}

In this work, the ion-exchange properties of antimony silicate, antimony titanate, and titanium tungstate based materials with a pyrochlore structure were studied. Abe et al.¹⁷ had synthesized titanium antimonates by hydrolysis at 60 °C, but these materials were of the rutile structure type. Qureshi et al.¹⁸ precipitated titanium tungstates at room temperature that were amorphous; therefore, the determination of the ion-exchange properties related to the structures of these materials is impossible. The uptake of ⁸⁵Sr, ¹³⁴Cs, and ⁵⁷Co by antimony silicates doped with Ti⁴⁺, Nb⁵⁺, Mo⁶⁺, and W⁶⁺ was studied in an earlier work.¹⁹

An attempt to tailor the ion-exchange properties of the metal oxide pyrochlores was conducted by the elemental substitution of some of the metals in the framework with W⁶⁺, Sb⁵⁺, and Nb⁵⁺. The addition of an element with a high charge was expected to increase the acidity of the exchanger, which is needed for it to function efficiently in acidic solutions. A possible defect in the structure created by incomplete substitution (vacancy)¹² may also lead to a structural charge in the material, in a similar manner as the Al/Si ratio in zeolites, thus affecting the ion-exchange properties. However, the focus of this work was to study the ion-exchange properties mainly as a function of the lattice parameter of the cubic unit cell.

Experimental Section

All reagents were of analytical grade, obtained from commercial sources, and used without further purification. The radioactive tracers were obtained from Amersham International (UK).

(12) Subramanian, M. A.; Aravamudan, G.; Subba Rao, G. V. *Prog. Solid State Chem.* **1983**, *15*, 55.

(13) Hervieu, M.; Michel, C.; Raveau, B. *Bull. Soc. Chim. Fr.* **1971**, *11*, 3939.

(14) Groult, D.; Michel, C.; Raveau, B. *J. Inorg. Nucl. Chem.* **1974**, *36*, 61.

(15) Rocha, J.; Amerson, M. W. *Eur. J. Inorg. Chem.* **2000**, 801.

(16) Behrens, E. A.; Poojary, D. M.; Clearfield A. *Chem. Mater.* **1998**, *10*, 959.

(17) Abe, M.; Chitrakar, R.; Tsuji, M.; Fukumoto, K. *Solvent Extr. Ion Exch.* **1985**, *3* (1–2), 149.

(18) Qureshi, M.; Gupta, J. P. *J. Chem. Soc. A* **1969**, 1755.

(19) Möller, T.; Harjula, R.; Pillinger, M.; Dyer, A.; Newton, J.; Tusa, E.; Amin, S.; Webb, M.; Araya, A. *J. Mater. Chem.* **2001**, *11* (5), 1526.

Characterization. X-ray diffraction (XRD) patterns were collected using a Scintag PAD-V operating at 40 kV and 30 mA. An internal silicon standard and a TREOR refinement program were used in the unit cell dimension determinations. The water content in each sample was determined by thermogravimetry (TGA) by using a Dupont Thermal Analyst 2000 system at a heating rate of 10 °C min⁻¹ under nitrogen. The elemental analyses of the materials were performed by direct-coupled plasma–atomic emission spectroscopy (DCP-AES) with a SpectraSpan VI spectrometer (error of determination <3%). About 50 mg of the sample was dissolved with 0.8 g of NaOH pellets in a platinum crucible at 585 °C. The melt was dissolved in deionized water and acidified with 6 mL of concentrated HCl after which 1 mL of 30% H₂O₂ was added and the sample was diluted to 100 mL with deionized H₂O. The determinations of alkali and alkaline earth metal concentrations in the ion-exchange experiments were carried out by atomic absorption spectroscopy (AAS) on a Varian Spectra AA-300 spectrometer. Approximate particle size determinations were done with Zeiss DSM 962 scanning electron microscope (SEM).

Synthesis of the Mixed Metal Oxide Pyrochlores. The pyrochlores were prepared as described in more detail elsewhere:²⁰ (1) precipitation by hydrolysis at pH < 1 in ~1.48 M HCl at 55 or 77 °C and (2) hydrothermal reaction at 150–190 °C at neutral pH in the presence of 0.06–0.5 M urea.

The antimony silicate was prepared by carefully mixing SbCl₅ (99%) in 4 M HCl with silicate solution (Ludox AS-40) in a 1:1 mole ratio and then adding deionized water (final concentration of acid is 1.48 M) in a plastic container. The reaction mixture was then left standing in a 77 °C oven for 1 day (sample SbSi1). Tungsten and niobium were introduced as dopants through the addition of an aqueous solution of Na₂WO₄·2H₂O or NbCl₅ (99%) to the mixture with a W/Sb (SbSiW1) or Nb/Sb (SbSiNb1) mole ratio of 0.1. The resulting white precipitates were filtered, washed with deionized water, and dried at 65 °C. The same procedure was followed in the preparation of antimony titanate doped with tungsten.

The hydrothermal syntheses of the titanium tungstates were carried out in the presence of urea. Urea slowly raises the pH of the reaction through the acidic hydrolysis of CH₄N₂O, which results in the formation of ammonia. A Ti/W mole ratio of 0.5 was used in the reactions for SbTiW2, NbTiW1, and NbTiW2, and that of 0.44 was used for TiW2. Antimony was introduced into the reaction of SbTiW2 in a Sb/W mole ratio of 0.05, and niobium was introduced to NbTiW1 and NbTiW2 in Nb/Ti mole ratios of 0.01 and 0.1, respectively. The mixtures were transferred into Teflon-lined pressure vessels that were placed in 150 or 190 °C ovens for 5–6 days. An antimony tungstate was prepared in a similar manner at 190 °C with a Sb/W molar ratio of 2 (sample SbW1).

Ion-Exchange Experiments. Indication of the selectivity of the ion exchanger can be obtained from the determination of the distribution coefficient (*K_D*).²¹ Therefore, the synthesized products were first evaluated by measuring the ⁸⁹Sr and ¹³⁷Cs *K_D* values by the batch method in 0.1 M HNO₃ and 0.1 M NaNO₃. The solutions were traced with a radioactive isotope and equilibrated with the ion exchanger in 20 mL polyethylene vials (Kimble), with a solution volume to exchanger mass ratio of 100–400 mL g⁻¹ for 1–3 days at ambient temperature, using constant rotary mixing. The solids were then separated from the solutions by filtration through 0.22 μm Minispike PVDF Bulk Acrodisk 13 filters. Aliquots of 2 mL each of the filtrates were measured for the ¹³⁷Cs and ⁸⁹Sr activities with a Wallac 1410 liquid scintillation counter. The pH values of the sample solutions were measured after equilibration with the exchanger.

The inactive sorption experiments were carried out in a similar manner by equilibrating the exchanger with a 0.001 M metal salt solution (MNO₃, M(NO₃)₂, MCl, or MCl₂, where

(20) Möller, T.; Clearfield, A.; Harjula, R. Submitted to *Microporous Mesoporous Mater.*

(21) Helfferich, F. G. *Ion Exchange*; Dover Science: Mineola, NY, 1995.

Table 1. Unit Cell Dimensions, a (Å), of Metal Oxide Pyrochlores in H^+ , NH_4^+ , and Ca^{2+} Forms

sample code	molar ratio of elements in product	H^+ form from synthesis	NH_4^+ form from synthesis	H^+ form after 0.1 M HNO_3	Ca^{2+} form after 0.1 M $Ca(NO_3)_2$
SbSi1	0.7:1	10.3914(16)		10.4041(31)	a
SbSiW1	0.7:1:0.04	10.3407(10)		10.3593(15)	10.2926(28)
SbSiNb1	0.87:1:0.01	10.3891(18)		10.4024(17)	10.2618(12)
SbTiW1	0.4:1:0.02	10.4207(17)		10.4387(29)	10.3856(9)
SbTiW2	0.09:1:0.95		10.2710(9)	10.2824(7)	a
NbTiW1	0.02:1:0.92		10.2591(9)	10.2758(14)	a
NbTiW2	0.1:1:0.57		10.2574(11)	10.3213(32)	10.2886(11)
TiW2	1:0.93		10.2656(7)	10.3142(34)	a
SbW1	1:0.6		10.3164(32)	a	a

^a Not determined.

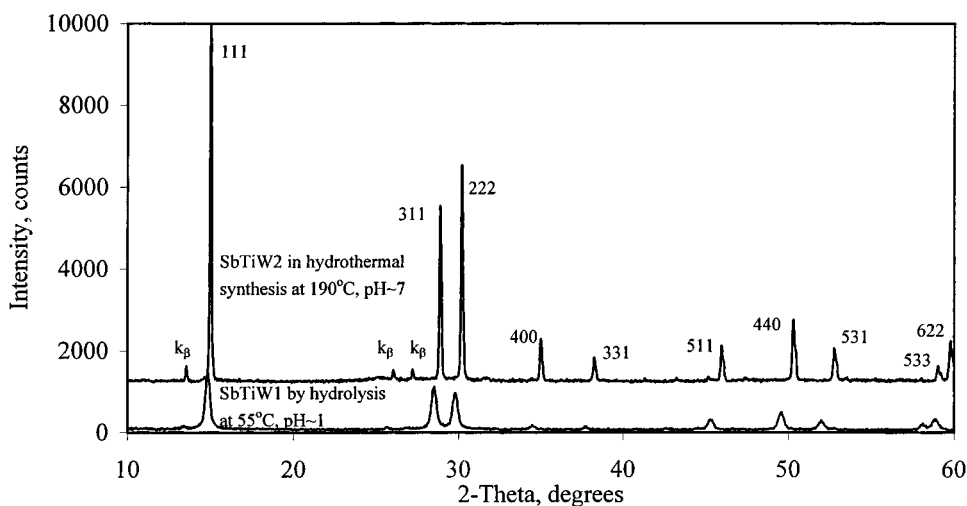


Figure 1. Powder XRD traces of a W-doped antimony titanate prepared by hydrolysis (SbTiW1) and a Sb-doped titanium tungstate synthesized hydrothermally (SbTiW2).

$M = Na^+, K^+, Rb^+, Cs^+, Mg^{2+}, Ca^{2+}, Sr^{2+},$ or Ba^{2+}). The element concentrations in solution were measured by AAS, and distribution coefficient (K_D) values were calculated as before.²⁰

For the ion-exchange experiments, the samples were converted to proton, sodium, and calcium forms in successive batch equilibrations. Materials that were synthesized in the NH_4^+ form (in the presence of urea) were first calcined at 400 °C (heating rate of 5 °C min^{-1}) to remove the NH_3 molecule. It has been noted earlier that calcination at ≤ 400 °C does not destroy the ion-exchange capacity of these kinds of materials.²² To obtain the H^+ form, 0.5–1.0 g of exchanger was equilibrated with 20 mL of 0.1 M HNO_3 . Fresh HNO_3 was changed several times until a pH of about 1.3 was reached. To obtain the Na^+ form, 0.2 g of the sample was equilibrated with 50 or 100 mL of 1 M $NaNO_3$. A fresh solution was changed eight times. After the fifth equilibration, a solution of 0.1 M $NaNO_3$ with 0.01 M $NaOH$ was used to ensure more complete conversion at higher pH (~ 11.5). The last two equilibrations were carried out with 1 M $NaNO_3$, again with a final pH of 8.5–9.5. Finally, the samples were washed quickly with deionized water and dried at 60 °C. To obtain the Ca^{2+} form of the material, the sample was shaken with 0.01 M $Ca(NO_3)_2$ ($BF = 100$) in 11 successive equilibrations and finally 3 times with 1 M $Ca(NO_3)_2$. The products were quickly washed with deionized water and dried at 60 °C. Powder XRD traces were run for each sample to ensure that destruction of the structure had not occurred.

Results

The mixed metal oxides under study were isostructural and of the cubic pyrochlore structure type ($Fd\bar{3}m$). The determining factors in the formation of the pyro-

chlore structure are, in addition to the appropriate element and charge combination, the pH and temperature of the reaction.²⁰ The crystallinity of the products prepared hydrothermally was usually better than that of the ones synthesized by precipitation. The powder XRD traces of a tungsten-doped antimony titanate, prepared by hydrolysis at 55 °C (SbTiW1), and an antimony-doped titanium tungstate, synthesized hydrothermally (SbTiW2), showed (Figure 1) that SbTiW2 was clearly more crystalline than SbTiW1. The compositions²⁰ of the products under study are given in Table 1. The SEM images showed that the crystalline materials had a well-defined morphology with octahedral and cubelike particles that were 1–2 μm in size. On the other hand, a sample prepared by precipitation (SbSiW1) consisted of large particles ($< 100 \mu m$) that were more irregular in shape but resembled cubes. Also present were small irregular platelets which is in correlation with the lower crystallinity of the compound.

Ion-Exchange Properties. The rigid three-dimensional framework of the pyrochlore does not undergo substantial dimensional change when exchanged to a different cationic form. However, some structural distortion was observed, which is contingent upon the degree of dehydration and the nature of the exchanging cation. The unit cell dimensions of the product in the NH_4^+ form were slightly smaller (0.2–0.6%) than that of the H^+ form (Table 1) in correlation with the radii of the hydration shells of NH_4^+ (2.13 Å) and H_3O^+ (3.3 Å). Dehydration of the materials, by heating to 400 °C, resulted in a shift of the peaks to lower angles in the

(22) Harjula, R.; Möller, T.; Amin, S.; Dyer, A.; Pillinger, M.; Newton, J.; Tusa, E.; Webb, M. International Patent Application WO 99/59161, 1999.

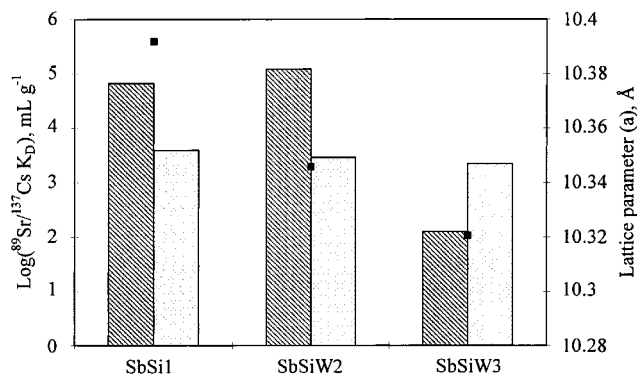


Figure 2. Effect of the lattice parameter (a , ■) on the ^{89}Sr (striped bar) and ^{137}Cs (dotted bar) distribution coefficients (K_D) in 0.1 M HNO_3 of antimony silicate pyrochlore SbSi1 and W-doped pyrochlores SbSiW2 and SbSiW3.

XRD patterns, which would indicate that the removal of the NH_3 molecule led to a slight relaxation of the structure. A similar trend has been observed by Grout et al.¹⁴ Again, as a result of conversion to the Ca^{2+} form from the H^+ form, the unit cell decreased in size (change in a was 0.3–1.2%) as expected because of the higher positive charge of the calcium ion (Table 1). Changes of about 0.8% in the lattice parameters have been observed for the crystalline antimony pentoxide in the proton form when it was ion-exchanged with the alkali metals.¹

Differences of about 1.5% in the unit cell dimensions were obtained with elemental substitutions into the structure, even with elements of similar size such as Sb^{5+} , Ti^{4+} , Nb^{5+} , and W^{6+} ($r = 0.60 \pm 0.04$ Å). The smallest lattice parameter ($a = 10.2591(9)$ Å) was observed with a Nb-doped titanium tungstate (NbTiW1) in the ammonium form that increased to 10.2758(14) Å upon conversion to the H^+ form (Table 1). The largest unit cell, 10.4387(29) Å, was obtained with the W-doped antimony titanate (SbTiW1) in the H^+ form. The antimony silicate SbSi1 has a lattice parameter (10.3914(16) Å) that is very close to that of the antimony pentoxide, 10.38 Å. Therefore, it could be assumed that Si^{4+} ($r = 0.4$ Å) is substituted at the A site in the pyrochlore $\text{A}_2\text{B}_2\text{O}_6\text{O}'$ and does not play an important part in the building of the basic structure.

The effect of the unit cell dimensions on the uptake of ^{89}Sr and ^{137}Cs in 0.1 M HNO_3 was first studied with antimony silicate (SbSi1) and antimony silicates that were doped with tungsten (SbSiW2, SbSiW3). SbSiW2 and SbSiW3 had lattice parameters of 10.3457(28) and 10.3206(34) Å, respectively, in the NH_4^+ form. This "screening test" showed that the size of the unit cell might indeed have some effect on strontium uptake, as a clear increase in the distribution coefficient (K_D) values of ^{89}Sr in acid was observed when $a > 10.34$ Å (Figure 2). A similar phenomenon was seen with a more extensive study with eight pyrochlores in 0.1 M NaNO_3 (Figure 3). A jump in the ^{89}Sr K_D was seen again between 10.32 and 10.36 Å, and the value increased from 160 to 72 400 mL g^{-1} . This further verified that pyrochlores with $a > 10.34$ Å have a higher affinity for strontium. The final pH of the NaNO_3 solution equilibrated with the samples was 3–4, which is low enough for strontium to be present only as a Sr^{2+} ion.

The titanium tungstates showed higher affinity for cesium than strontium in 0.1 M HNO_3 (Table 2), and

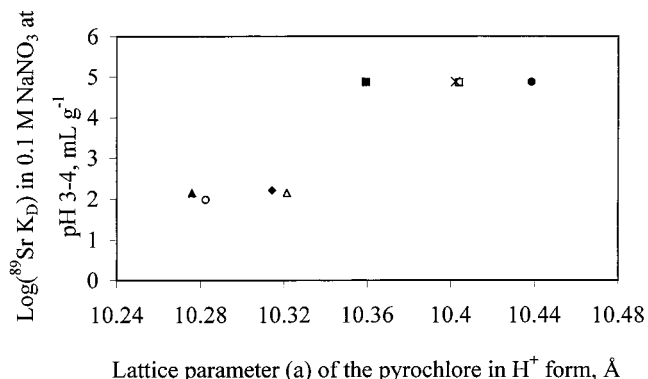


Figure 3. ^{89}Sr distribution coefficient (K_D) in 0.1 M NaNO_3 as function of the lattice parameter (a) of pyrochlores in the H^+ form (SbSi, □; SbSiW1, ■; SbSiNb1, ×; SbTiW1, ●; SbTiW2, ○; TiW2, ◆; NbTiW1, ▲; NbTiW2, △).

Table 2. ^{89}Sr and ^{137}Cs Distribution Coefficients (K_D) for the Metal Oxide Pyrochlores

sample code	^{137}Cs K_D , mL g^{-1}		^{89}Sr K_D , mL g^{-1}	
	0.1 M HNO_3	0.1 M NaNO_3	0.1 M HNO_3	0.1 M NaNO_3
SbSi1	3930 ± 30	11 ± 1	66 400 ± 1000	47 700 ± 700
SbSiW1	4200 ± 30	39 ± 1	178 100 ± 3600	55 400 ± 800
SbSiNb1	8210 ± 60	22 ± 1	358 000 ± 8000	60 200 ± 900
SbTiW1	290 ± 2	69 ± 1	90 ± 1	585 ± 4
SbTiW2	2490 ± 20	11 ± 1	36 ± 1	1340 ± 10
NbTiW1	2287 ± 15	468 ± 3	13 ± 1	6200 ± 40
NbTiW2	4850 ± 35	2230 ± 15	16 ± 1	3990 ± 30
TiW1	18 330 ± 180	480 ± 3	39 ± 1	651 ± 5
TiW2	19 700 ± 200	529 ± 4	174 ± 1	^a
TiW3	11 365 ± 115	380 ± 3	51 ± 1	905 ± 6

^a Not measured.

the amount of tungsten was found to be an important factor in creating cesium selectivity in these pyrochlores (Table 2). Reasonably high ^{137}Cs K_D values of 18 300 and 19 700 mL g^{-1} were obtained with samples TiW2 and TiW1, respectively. The W/(Ti + W) ratio in TiW2 and TiW1 was 0.48 and 0.35, respectively. When the amount of tungsten was higher, the ^{137}Cs K_D value started to decrease slightly, with a value of 11 400 mL g^{-1} for TiW3 (W/(Ti + W) = 0.6). On the other hand, the increase of titanium in the product led to a phase change, and sample TiW4, with W/(Ti + W) = 0.26, was not a pure pyrochlore. The powder XRD pattern showed the presence of a TiO_2 (anatase) impurity phase. With further increase of titanium, anatase became the dominant phase (TiW5). The effect of the unit cell dimensions on cesium selectivity of these titanium tungstates was not clear because of the small difference in the lattice parameters of TiW1, TiW2, and TiW3 (10.2656–10.3000 Å) and the ^{137}Cs distribution coefficients in 0.1 M HNO_3 . However, the ^{137}Cs K_D values obtained in 0.1 M NaNO_3 (380–530 mL g^{-1}) were almost 2 orders of magnitude lower than those in acid (Table 2), which indicated that the smaller Na^+ ion is preferred over Cs^+ . Again, this is evidence of the ion sieve character of the pyrochlore structure. If the titanium tungstate was doped with niobium, the selectivity for cesium in the presence of macro component sodium could be improved and a ^{137}Cs K_D value of 2230 mL g^{-1} in 0.1 M NaNO_3 was obtained for NbTiW2 (Table 3). Therefore, in addition to the unit cell dimensions, the element substituted into the framework affects the selectivity and capacity of the exchanger by altering the acidity of the exchanger.

Table 3. Distribution Coefficients (K_D) of Alkali and Alkaline Earth Cations for the Metal Oxide Pyrochlores in the H^+ Form^a

sample code	$K_D(Na^+)$ mL g ⁻¹	$K_D(K^+)$ mL g ⁻¹	$K_D(Rb^+)$ mL g ⁻¹	$K_D(Cs^+)$ mL g ⁻¹	$K_D(Mg^{2+})$ mL g ⁻¹	$K_D(Ca^{2+})$ mL g ⁻¹	$K_D(Sr^{2+})$ mL g ⁻¹	$K_D(Ba^{2+})$ mL g ⁻¹
SbSi1	14 170 ± 990	12 250 ± 860	13 340 ± 930	115 ± 10	215 ± 15	3048 ± 15	6860 ± 480	5700 ± 400
SbSiW1	3480 ± 240	1460 ± 100	3740 ± 260	250 ± 20	14 190 ± 990	34 300 ± 2400	23 800 ± 1700	60 900 ± 4300
SbSiNb1	6580 ± 460	19 270 ± 1350	5580 ± 390	280 ± 20	300 ± 20	1550 ± 110	2310 ± 160	3010 ± 210
SbTiW1	670 ± 50	1680 ± 120	640 ± 50	26 ± 2	9 ± 1	112 ± 10	260 ± 20	1365 ± 95
SbTiW2	91 ± 6	1300 ± 90	295 ± 20	15 ± 1				
NbTiW2	34 ± 2			107 ± 10	9 ± 1	15 ± 1	45 ± 3	165 ± 12
TiW2		1560 ± 110	220 ± 15		14 ± 1	13 ± 1	45 ± 3	148 ± 10

^a pH at equilibration is 3–4.

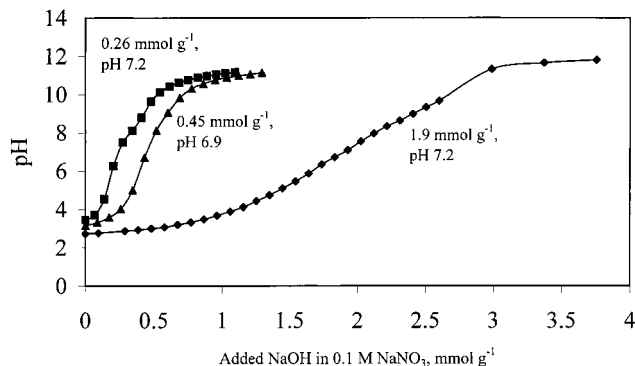


Figure 4. Titration curves in 0.1 M NaNO₃ of W-doped antimony titanate pyrochlores in the H^+ form (SbTiW1, ◆; SbTiW2, ■; SbTiW3, ▲).

Titration of the pyrochlores with varying amounts of Sb⁵⁺, Ti⁴⁺, and W⁶⁺ in the lattice clearly showed the effect of substitution on capacity (Figure 4). Samples SbTiW2 and SbTiW3 had high contents of W⁶⁺ and Sb⁵⁺, respectively, and the sharp inflections in the titration curves indicate that they are strongly acidic in nature. With high Ti⁴⁺ content and very little W⁶⁺ in SbTiW1 the exchanger is weakly acidic. However, SbTiW1 has the largest unit cell ($a = 10.4387(29)$ Å in H^+ form) as well as capacity, 1.9 mequiv g⁻¹ at pH 7.2, while SbTiW2 and SbTiW3 have smaller lattice parameters and H^+ capacities of <0.5 mequiv g⁻¹ at pH ~ 7. Therefore, it would seem that in addition to selectivity, the lattice parameter has a significant effect on the capacity of these pyrochlores. The ion-exchange capacity of the titanium antimonate of the rutile structure has been similarly found to be dependent on the antimony content.²³ The titrations were carried out with an automatic titrator and do not represent an equilibrium situation in the exchangers. Therefore, the true capacities of the materials could be slightly higher than the ones given here, since equilibrium is achieved at longer times than in the dynamic method.

Selectivity for Alkali and Alkaline Earth Cations. The effect of the unit cell size on the selectivity for alkali metals and alkaline earth metals in macro amounts was studied with seven samples of which the lattice parameters varied between 10.28 and 10.44 Å in the H^+ form (Figures 5 and 6 and Table 3). At ~10.32 Å (samples NbTiW2 and TiW2), the alkali metal selectivity series followed Eisenman's selectivity series VI, $K^+ > Na^+ > Rb^+ > Cs^+$. A similar trend was observed for pyrochlores with $a \approx 10.40$ Å (SbSi1 and SbSiNb1) and $a \approx 10.44$ Å (SbTiW1). This trend is typical for

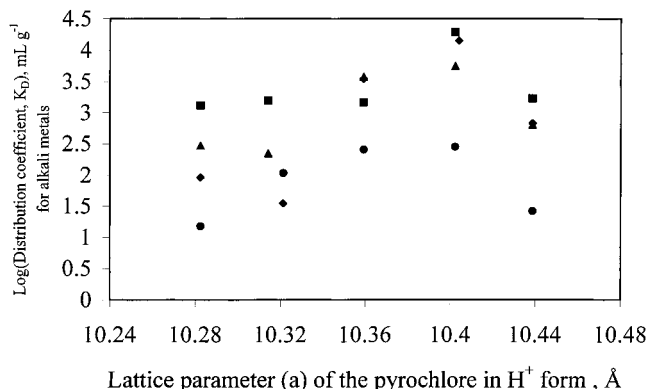


Figure 5. Distribution coefficients of the alkali metals Na⁺ (◆), K⁺ (■), Rb⁺ (▲), and Cs⁺ (●) as a function of the lattice parameter of pyrochlores in the H^+ form.

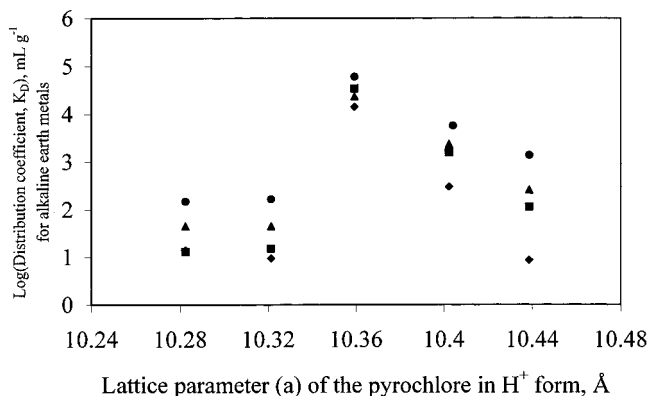


Figure 6. Distribution coefficients of the alkaline earth metals Mg²⁺ (◆), Ca²⁺ (■), Sr²⁺ (▲), and Ba²⁺ (●) as a function of the lattice parameter of pyrochlores in the H^+ form.

inorganic ion exchangers with medium charge density. The antimony pentoxide, the structural analogue of these pyrochlores, is known to prefer Na⁺ over Cs⁺ as well.

It is difficult to make correlations between the lattice parameter and the selectivity in this situation, as the hydration energies of the in-going cations have to be considered in addition to the change in acidity of the exchanger with the substitution of a more acidic element into the framework. However, a jump in Na⁺ and Rb⁺ K_D values at $a > 10.32$ Å (Figure 5) as well as in the alkaline earth cation uptake (Figure 6) would indicate that the size of the unit cell has a significant effect on the selectivity of these pyrochlores. In the case of cesium, the situation is different as the three-dimensional tunnel system of the pyrochlore framework clearly creates steric hindrances for the large cesium cation. Cs⁺ was taken up the least of the alkali metals

(23) Tsuji, M.; Kaneko, H.; Tamaura, Y. *J. Chem. Soc., Faraday Trans. 1993*, 89 (5), 851.

regardless of the unit cell parameter. It cannot be concluded as to whether the tunnels are too small for the cesium ion to enter or if its diffusion rate is slower than those of the smaller ions without more accurate characterizations of the structures and study of the kinetics in more detail.

A rational selectivity series was observed for the alkaline earth metals that followed the reverse order of the second group, $\text{Ba}^{2+} > \text{Sr}^{2+} \approx \text{Ca}^{2+} > \text{Mg}^{2+}$ (Figure 6). As observed in the preliminary experiments with ^{89}Sr in 0.1 M HNO_3 and 0.1 M NaNO_3 (Figures 2-3), very little uptake of the cations occurred when the lattice parameter was $a < 10.32 \text{ \AA}$. A clear jump in the alkaline earth metal distribution coefficients was seen between 10.32 and 10.36 \AA too. The difference between Figures 3 and 6 is that in the case of the trace ^{89}Sr uptake in 0.1 M NaNO_3 , the distribution coefficient remained high with the increase of the unit cell dimension, while for a situation when strontium was present in macro amounts (10^{-3} M), the K_D decreased already at $a = 10.40 \text{ \AA}$. This discrepancy can be explained by the resulting conversion of the exchanger into the Na^+ form in NaNO_3 (Figure 3) and into the Sr^{2+} form in 0.001 M $\text{Sr}(\text{NO}_3)_2$. When strontium is present in macro concentrations, the H^+ pyrochlore is slowly being converted to the Sr^{2+} form, which causes its unit cell to decrease in a similar way as when converted to the Ca^{2+} form (Table 1). The lattice parameter of SbSiNb1 decreased from 10.4024(17) \AA in the H^+ form to 10.2618(12) \AA in the Ca^{2+} form. This value was already found to be unfavorable for effective strontium uptake. In 0.1 M NaNO_3 with trace strontium (^{89}Sr), the conversion in cationic form is to the Na^+ form, which does not cause as large a change in the unit cell size as the conversion to a cation form of bivalent state. Therefore, in the conditions where strontium was present in trace amounts, it could still be taken up efficiently at $a > 10.40 \text{ \AA}$. Again, the full explanation may not be as straightforward because of the several different factors that take part in creating selectivity in inorganic ion exchangers.

Relative to a titanosilicate of cubic structure, an analogue of the mineral pharmacosiderite ($a \approx 7.8 \text{ \AA}$),²⁴ these pyrochlores compare very well with regard to the cation uptake efficiency (Table 3). The most significant discrepancy is the higher cesium selectivity of the pharmacosiderites. The advantage in some of the pyrochlores is that they are more acidic and therefore function at a lower pH than the titanosilicates.

The relative selectivity between the different alkaline earth cations was rather low in general, which does not allow for their selective individual separation. Only a slight separation of magnesium from Ba^{2+} , Sr^{2+} , and Ca^{2+} was seen with the enlargement of the unit cell. It is presumed that this results from the hydration shell of Mg^{2+} most likely being too tightly bound to be stripped by the metal oxide framework, thus preventing the entrance of magnesium. Some of the materials showed high selectivity for the alkaline earths against the H^+ ion, making them suitable for removal of these cations from acidic solutions. However, they would not be selective enough for the efficient removal of strontium from nuclear waste effluents that contain calcium.

Conclusions

The relationship between the lattice parameter of the cubic unit cell and the ion-exchange properties of a group of mixed metal oxide pyrochlores was under study. An attempt to tailor the ion-exchange properties of the two-element materials was carried out by substituting a third element into the structure. Some consistency was seen in the relationship between the structure, selectivity, and capacity of these tunnel-type ion exchangers. A clear increase in cation uptake was observed when the lattice parameter was $> 10.34 \text{ \AA}$. However, the cationic form of the pyrochlore has a significant effect on the lattice parameter in this region and conversion to the Ca^{2+} or the Sr^{2+} forms caused the unit cell to become smaller, thus preventing further efficient uptake of Sr^{2+} . The situation was different in the case of cesium, which was taken up rather poorly, because the three-dimensional tunnel system of the pyrochlore framework creates steric hindrances for this large cation. Interestingly, the titanium tungstates showed reasonable affinity for ^{137}Cs in 0.1 M HNO_3 when the $\text{W}/(\text{Ti} + \text{W})$ ratio was 0.36–0.48. Although some of the materials showed high selectivity for the alkaline earths at low pH, their individual separation from each other by these pyrochlores was low.

The other factors that influence the exchange properties, such as the stronger acidity of the exchanger caused by a more acidic element in the structure (W^{6+} , Sb^{5+}) and the hydration energy of the exchanging cation, should be taken into account to fully understand the ion-exchange behavior of these materials. In the W-doped antimony titanates, the effect of the acidic element in the structure on the ion-exchange properties was clearly observed. The titanium tungstate based compound (high W^{6+} content) was the most acidic compound as shown by the sharp inflection in the titration curve (Figure 4), but it had the lowest capacity. The antimony titanate with low tungsten content was weakly acidic but had the largest unit cell as well as the highest H^+ capacity.

It is now essential for this work to solve the structures of these pyrochlores in detail to fully understand their ion-exchange behavior. The investigation of pyrochlores with $a > 10.44 \text{ \AA}$ could also be of interest. It is assumed that this could be achieved by the substitution of cations of bigger size into the framework, such as Zr^{4+} . The incorporation of elements with several oxidation states, like nickel and cobalt, into the pyrochlore structure could also prove to give materials with interesting ion-exchange properties.

Acknowledgment. This work was supported by Lockheed Martin Energy Systems, Inc. (through Grant #9800585), Oak Ridge National Laboratory, and DOE Basic Energy Science (Grant #DE-FG07-96ER14689) and funded by the Office of Environmental Management (EMSP) and the National Technology of Finland (TEKES 187/401/98). Support was also received from the Finnish foundations Imatran Voiman Säätiö (Fortum) and Ella ja Georg Ehrnroothin Säätiö. T.M. also thanks Dr. Joy Heising for assistance with the DCP-AES measurements as well as helpful discussions.

(24) Behrens, E. A.; Clearfield, A. *Microporous Mater.* **1997**, *11*, 65.